



Contents lists available at ScienceDirect

Journal of King Saud University – Science

journal homepage: www.sciencedirect.com

Original article

Suppression of cytokine storm and associated inflammatory mediators by salicylaldehyde derivative of pregabalin: An innovative perspective for alleviating airway inflammation and lung remodeling

Muhammad Shoaib Zafar^a, Khadija Shahid^b, Glenda C. Gobe^{c,d}, Riffat Yasmin^e, Nadia Naseem^f, Muhammad Shahzad^{a,*}^a Department of Pharmacology, University of Health Sciences, Lahore 54600, Pakistan^b Riphah International University, Islamabad 46000, Pakistan^c Faculty of Medicine, University of Queensland, Brisbane 4006, Queensland, Australia^d Kidney Disease Research Collaborative, Princess Alexandra Hospital and University of Queensland, Translational Research Institute, Brisbane 4102, Queensland, Australia^e Riphah International University, Faisalabad 38000, Pakistan^f Department of Morbid Anatomy and Histopathology, University of Health Sciences, Lahore 54600, Pakistan

ARTICLE INFO

Article history:

Received 3 October 2021

Revised 9 January 2022

Accepted 26 January 2022

Available online 2 February 2022

Keywords:

Pregabalin

Salicylaldehyde

Airway inflammation

Lung remodelling

Inflammatory mediators

ABSTRACT

Objectives: Pregsal is a novel salicylaldehyde derivative of pregabalin, a structural analogue of gamma-aminobutyric acid approved for treating epilepsy, neuropathic pain and diabetic peripheral neuropathy but not trialled to date for airway inflammatory diseases. The current study evaluated a preclinical model of airway inflammation and lung remodelling induced by ovalbumin (OVA) for the potential benefits of pregal.

Methods: Wistar rats (N = 10 per group) were divided into four groups sensitized intraperitoneally (i.p.) and then challenged intranasally with OVA, with or without i.p. pregal (100 mg/kg) or methylprednisolone (MP) (15 mg/kg). Airway inflammation was assessed through inflammatory cell infiltration in the lungs, delayed-type hypersensitivity (DTH), and nitric oxide (NO) level using bronchoalveolar lavage fluid (BALF) and lung tissues. The mRNA expression levels of a panel of inflammatory mediators (cytokines, chemokine and growth factors) in the lungs were measured by the reverse transcription-polymerase chain reaction (RT-PCR). Systemic inflammation was assessed using splenocyte proliferation and total and differential leucocyte count in blood and BALF. Lung remodelling was assessed by wet/dry lung weight ratio, epithelial thickness and goblet cell hyperplasia, hydroxyproline and osteopontin (OPN) levels, arginase activity in lungs, and ornithine decarboxylase (ODC) activity in lung mitochondria.

Results: Pregsal significantly alleviated the total and differential leucocyte count in blood and BALF, NO production in BALF and recruitment of inflammatory cells in the lungs. It suppressed the T-cell response and attenuated the OVA-induced lung epithelial thickness, goblet cell hyperplasia, wet/dry lung weight ratio, hydroxyproline and OPN levels, arginase and ODC activity. Levels of inflammatory mediators were also downregulated in the lungs by pregal.

Conclusions: The key findings of this study indicate that pregal significantly reduces the development of airway inflammation and lung remodelling by suppression of cytokine storm and associated inflammatory mediators.

© 2022 Published by Elsevier B.V. on behalf of King Saud University. This is an open access article under the CC BY-NC-ND license (<http://creativecommons.org/licenses/by-nc-nd/4.0/>).

* Corresponding author Tel #: 0092-334-6061838.

E-mail addresses: shahzad912@hotmail.com, shahzad912@uhs.edu.pk (M. Shahzad).

Peer review under responsibility of King Saud University.



Production and hosting by Elsevier

1. Introduction

Acute and chronic airway inflammation occurs when the immune system responds to an infection or allergy. Such a situation seems currently in severe acute respiratory syndrome coronavirus-2 (SARS-CoV-2), where an over-activated innate immunity is a potential pathological mechanism (Liu et al., 2020). SARS-CoV-2 mediates damage in the lungs through exten-

<https://doi.org/10.1016/j.jksus.2022.101877>

1018-3647/© 2022 Published by Elsevier B.V. on behalf of King Saud University.

This is an open access article under the CC BY-NC-ND license (<http://creativecommons.org/licenses/by-nc-nd/4.0/>).

sive secretion of cytokines, chemokines and reactive oxygen species that may directly damage the lungs. The outcome is pulmonary edema, hyaline membrane formation and desquamation of alveolar cells (Xu et al., 2020).

More commonly, however, asthma also results in bronchial hyper-responsiveness with reversible structural changes in airway remodelling. The airway inflammation associated with bronchial asthma is accompanied by the accumulation of acute and chronic inflammatory cells, such as neutrophils, lymphocytes, eosinophils, macrophages and T-cells in the airways (Lambrecht and Hamad, 2015). In chronic asthma, persistent airway inflammation causes hypertrophy of mucus glands, airway smooth muscle cells, overproduction of mucus by goblet cells in lungs, subepithelial fibrosis and thickening of the airway walls. Thus, the development of airway inflammation and subsequent lung remodelling is the main pathological features in acute and chronic lung conditions, irreversible lung remodelling characterized by narrowing of the airways and airflow limitation is more commonly seen with chronic asthma and chronic obstructive pulmonary disease (Hirota and Martin, 2013).

Novel therapeutic approaches are required to attenuate airway inflammation and lung remodelling. Inhaled corticosteroids, alone or in combination with short-acting and long-acting β_2 -adrenoreceptor agonists, are generally used to manage airway inflammation and airway remodelling (McCracken et al., 2017). The use of corticosteroids is unable to reverse lung remodelling and their long-term use causes side effects such as immunosuppression and predisposing patients to lung infection with opportunistic micro-organisms. Researchers have also found that inhaled corticosteroids are not beneficial for all asthmatic patients and many patients are resistant to standard corticosteroid therapy (Barnes, 2013). Similarly, evidence suggests corticosteroids should be administered cautiously to COVID-19 patients, with strict limitations on indications and dosage (Russell et al., 2020).

Pregabalin is a structural analogue of gamma-aminobutyric acid, which is a naturally occurring neurotransmitter but functionally unrelated, with potent anxiolytic, anticonvulsant and analgesic activity (El-Naby, 2019). Pregabalin also has bronchodilator activity and the potential to alleviate the symptoms of asthma (Schrier and Taylor, 2002). Previously, the synthesis of a salicylaldehyde derivative of pregabalin, pregsal, was reported, and dose-dependent (50, 75, 100 mg/kg) antipyretic, analgesic and anti-inflammatory activities were found (Ahmad et al., 2017).

In view of these effective pharmacological applications, the present study aimed to test whether pregsal would ameliorate airway inflammation and lung remodelling processes in preclinical ovalbumin (OVA)-induced rat model of airway inflammation via anti-inflammatory and immunomodulatory mechanisms.

2. Materials and methods

2.1. Experimental animals

The study was performed at the Department of Pharmacology, University of Health Sciences (UHS), Lahore, Pakistan. Male Wistar rats, 6 to 8 weeks old, weighing 200–230 g, housed under standard environmental conditions of humidity (50–60 %), temperature (23–25 °C), and 12:12 h light:dark cycle had free access to standard rat chow and water. The rats were acclimatized for 7 days without any intervention before the start of experiments. All the experimental procedures and handling of animals were approved by the Ethical Review Committee, UHS, Lahore; approval number UHS/1612.

2.2. Groups and dosage

Male rats were randomly divided into four groups, each N = 10. Group I (negative control, NC): Sham-sensitized intraperitoneally (i.p.) and intranasally challenged with phosphate-buffered saline (PBS). Group II (OVA): Sensitized i.p. and intranasally challenged with OVA to induce lung inflammation and remodelling. Group III (Pregsal): Sensitized i.p. and intranasally challenged with OVA and treated with pregsal through intraperitoneal injection at a dose of 100 mg/kg body weight 2 h before sensitization and challenge. Group IV (MP): Sensitized i.p. and intranasally challenged with OVA and treated with methylprednisolone (MP) at 15 mg/kg body weight through i.p. injection 2 h before sensitization and challenge.

2.3. Induction of lung inflammation and remodelling

To induce lung inflammation and remodelling, rats underwent i.p. sensitization, and then airways were challenged with OVA by nasal inhalation. Briefly, at day zero and fourteen, 200 μ l of a stock solution of 1 mg of OVA (Sigma-Aldrich, St Louis, MO) emulsified in 50 mg aluminum hydroxide (adjuvant) (AppliChem, Chemica Synthesis Services, Germany) were delivered in 1 ml PBS to all groups except NC. On the 21st day, one week after the second sensitization, intranasal OVA challenge (200 μ g OVA in 200 μ l PBS) was administered daily for fourteen days till day 35. Rats in the NC group were sensitized and challenged with PBS instead of OVA (Raza Asim et al., 2010).

2.4. Delayed-type hypersensitivity assay (DTH)

DTH is the basic *in vivo* analysis performed to confirm the inflammatory response to the antigen. An established assay for DTH was used (Ashraf et al., 2015). Briefly, 24 h before being euthanized, all rats were subcutaneously challenged with 20 μ l OVA (1 mg OVA dissolved in 1 ml PBS) in the pinna of the right ear, whereas the left ear was challenged with 20 μ l PBS (as control). Shortly after euthanization, the distance from the apex of the rat ears was measured, the right and left ears were cut from the same point and weighed by using a digital balance. The difference in weight of the right and left ears revealed the magnitude of DTH.

2.5. Inflammatory cells in the blood and bronchoalveolar lavage fluid (BALF)

On day 35, the rats of all the groups were anaesthetized using ether, and blood samples were collected in EDTA vacutainers after intra-cardiac puncture for hematological analysis. For collecting BALF, the trachea and lungs were removed from rats and lavaged X3 by gradual instillation and aspiration of 2 ml ice-cold PBS through the trachea using a 3 cc syringe with a blunt needle. BALF was centrifuged at 1500g for 10 min. The supernatant was stored for the determination of nitric oxide (NO), while the precipitate was resuspended in 1 ml ice-cold PBS. The total leucocyte count (TLC) and differential leucocyte count (DLC) were determined in the blood and BALF using an automated hematology analyzer (Sysmex XT-1800i).

2.6. Wet/dry lung weight ratio

Lung edema was determined through a wet/dry lung weight ratio. After euthanization, the complete left lung, with superior and inferior lobes, was excised, and wet weight was measured instantly. Then, the lung was dried for 15 min at 56 °C in the oven and weighed. For the determination of wet/dry lung weight ratio,

the wet lung weight was divided by the weight of dry lung (Rana et al., 2016).

2.7. Determination of nitric oxide (NO) in BALF

NO in BALF was determined using commercially available Griess reagent (Biotium, Fremont, CA, USA) as per the manufacturer's guidelines. The absorbance was recorded at a wavelength of 540 nm by a microplate reader (BioTek®, Synergy HTX).

2.8. Lung tissue histopathology

A lobe from the right lung was excised soon after collection of BALF, washed in ice-cold PBS and fixed with 10 % neutral buffered formalin. Using routine histological procedures, tissue was embedded in paraffin and sections cut at 5–6 µm. Haematoxylin and Eosin (H&E) staining of lung tissues is used to determine the bronchial epithelial wall thickening and infiltration of inflammatory cells. A semi-quantified inflammatory score was utilized by giving grades 0 = no inflammation, 1 = minimal inflammatory cells in some microscope fields; 2 = mild inflammation with an influx of 1–2 inflammatory cells in most microscope fields; 3 = moderate inflammation with 3–4 inflammatory cells in most microscope fields; and 4 = severe inflammation with > 4 inflammatory cells in most microscope fields (Dong et al., 2012). Micrometer analysis of epithelial cell thickness was performed under an optical microscope using a graded eyepiece lens. Sections from each animal were also stained with Periodic Acid-Schiff (PAS) to identify mucus-secreting goblet cells. A PAS grade was given according to the percentage of goblet cells in the bronchial epithelium: Grade 1, 2, 3 and 4 = <15% goblet cells, 15–25% goblet cells, 26–50% goblet cells and 51–75% goblet cells, respectively (Abdel Aziz et al., 2013). All the histopathological assessments and scores were carried out in a blinded fashion and verified independently by a pathologist.

2.9. Estimation of hydroxyproline in lungs

A hydroxyproline assay kit (Abcam, UK) was used to determine the total amount of collagen in the lungs. Absorbance was measured at 560 nm using a microplate reader (BioTek®, Synergy HTX).

2.10. Arginase activity

Arginase activity in lung homogenates was estimated by using commercially available QuantiChrom Arginase Assay Kit (BioAssay system, Hayward, CA, USA). Absorbance was recorded at 430 nm using a microplate reader (BioTek®, Synergy HTX). Arginase activity was calculated as the unit (U) per mg of protein. 1 U arginase activity = 1 µM of L-arginine to ornithine and urea per minute at 37 °C and pH 9.5.

2.11. Enzyme-linked immunosorbent assay (ELISA) for osteopontin

OPN in lung homogenate was measured by ELISA according to the kit manufacturer's protocol (GloryScienceCo., Ltd.). Absorbance was determined at 450 nm using a microplate reader (BioTek®, Synergy HTX).

2.12. Activity of ornithine decarboxylase in lung mitochondria

Mitochondria from lung tissues were isolated by a mitochondrial isolation kit for the tissue using the manufacturer's protocol (Abcam, UK). Ornithine decarboxylase (ODC) activity in lung mitochondria was determined by a commercially available ODC ELISA kit (GloryScienceCo., Ltd.) according to the manufacturer's instruc-

tions. Absorbance was measured at 426 nm by using a microplate reader (BioTek®, Synergy HTX).

2.13. Determination of mRNA expression levels

Conventional PCR was used to access mRNA expression levels of TNF-α, NF-κB, IL-4, IL-8, IL-13, arginase I, TGF-β, FGF2, CTGF and Ull. Total RNA was extracted from lung tissue using a commercially available GeneJET RNA Purification Kit (Thermo Scientific, USA). The purity of RNA and its yield were quantified using nanodrop (Thermo Scientific, USA). RevertAid First Strand cDNA Synthesis Kit (Thermo Scientific, USA) was used for the synthesis of cDNA. GAPDH was used as a reference. The primers were designed by using the online primer designing tool-NCBI-NIH. Sequences of primers can be found in Table 1.

2.14. OVA-induced splenocyte proliferation

Rat splenocytes were cultured as described previously, with modifications (Shahzad et al., 2009). The whole individual spleens were isolated shortly after the euthanization of rats and washed X3 with cold Hank's Balanced Salt Solution (HBS, 100 mg/ml streptomycin, and 100 U/ml penicillin). Spleens were then finely minced in 5 ml HBSS containing collagenase type II (1 mg/ml) and calcium. The digested spleen tissue was filtered through a cell strainer. An equal volume of RBC lysis buffer (Abcam, UK) was added then the suspension centrifuged at 1000g for 10 min. Cells were then washed X3 with PBS, centrifuged for 10 min at 1000g, and the cell pellet resuspended in cell culture medium (RPMI-1640) having glutamine, sodium pyruvate, 10% FBS, 50 U/ml penicillin, 50 µg/ml streptomycin. Cells were counted using an improved Neubauer hemacytometer. 5×10^4 splenocytes were seeded per well in 96-well flat-bottom plate along with 200 µl of cell culture medium and incubated in a CO₂ incubator at 37 °C for 24 h for acclimatization. Splenocytes were then treated with 100 µg/ml OVA (splenocyte proliferation stimulant) with or without 10 µM of pregalsal or 400 µg/ml of the reference drug (MP). 100 µM 5-bromo-2'-deoxyuridine (BrdU) dissolved in cell culture media was added followed by incubation for 24 h, then BrdU incorporation was terminated by aspirating the supernatant cell culture medium and adding 200 µl of fixative/denaturing solution, followed by incubation at 37 °C for 30 min then X3 buffer wash. 100 µl of the prediluted anti-BrdU antibody were added per well followed by incubation in a CO₂ incubator for 1 h followed by washing. 100 µl peroxidase goat anti-mouse IgG HRP conjugate were added per well and incubated at 37 °C for 30 min, followed by X3 buffer wash. After a final dH₂O wash, substrate solution was added, followed by room temperature incubation for 30 min in the dark. 100 µl of stop solution were added within 15 min, and absorbance measured at 450 nm using an ELISA reader (BioTek®, Synergy HTX).

2.15. Statistical analysis

The data were expressed as mean ± SD. Statistical analysis was performed using GraphPad Prism v8.0c. One way analysis of variance (ANOVA) was applied to compare the quantitative variables and to analyze the difference among all groups, followed by post hoc Tukey's test. The value of P < 0.05 was considered as statistically significant.

Table 1
Sequences and annealing temperature of primers.

Primers	Forward/Reverse	Sequence	Product size	Annealing temp (°C)	Cycles
TNF-α	Forward	5'-AAGCTGTCTTCAGGCCAACA-3'	233	59.2	35
	Reverse	5'-CCCGTAGGGCGATTACAGTC-3'			
NF-κB	Forward	5'-CAAGGAAGAGGATGTGGGGTT-3'	207	64.8	35
	Reverse	5'-AGCTGAGCATGAAGGTGGATG-3'			
IL-4	Forward	5'-AACACCACGGAGAACGAGCTCATC-3'	152	59.2	35
	Reverse	5'-AGTGAGTTCAGACCGCTGACACCT-3'			
IL-8	Forward	5'-CCACGCCACAAGTACTACTGAT-3'	392	58.8	37
	Reverse	5'-TGGTTCTCATGAGGGGTCTG-3'			
IL-13	Forward	5'-CCTGGAATCCCTGACCAACA-3'	184	59	40
	Reverse	5'-GTGGCCATAGCGGAAAAGTTG-3'			
Arginase I	Forward	5'-TATCGGAGCCCTTCTCTA-3'	189	55.6	35
	Reverse	5'-ACAGACCGTGGTTCTTAC-3'			
TGF-β	Forward	5'-ACCTGCAAGACCATCGACATG-3'	85	65.4	35
	Reverse	5'-CGAGCCTTAGTTGGACAGGAT-3'			
FGF2	Forward	5'-TCCAAAACCTGACCCGATCC-3'	563	58.9	40
	Reverse	5'-TCTTGCAGTAGACCCGCTTG-3'			
CTGF	Forward	5'-ATGGAGACATGGCGTAAAGC-3'	151	53.7	38
	Reverse	5'-TCCCACAGCAGTTAGGAACC-3'			
Ull	Forward	5'-GCATCTTACCCTGACCATAA-3'	399	57.2	40
	Reverse	5'-CCCAGAGAGAAGGACGATACC-3'			
GAPDH	Forward	5'-TCTCTGCTCCTCCCTGTCT-3'	229	58.3	35
	Reverse	5'-CTTGCCGTGGGTAGAGTCAT-3'			

3. Results

3.1. Effect of pregsal on inflammatory process

3.1.1. Pregsal decreased inflammatory cells in BALF and blood

TLC of rats sensitized and challenged with OVA was significantly increased in BALF and blood compared with the NC group. Treatment with pregsal and MP significantly reduced TLC. Similarly, numbers of lymphocytes, neutrophils, eosinophils, monocytes and basophils in both BALF and blood of OVA groups were increased considerably over the NC group, and pregsal modulated this increase significantly (Table 2).

3.1.2. Pregsal reduced nitric oxide (NO) production in BALF

Enhanced NO production is considered as a marker of lung inflammation. The significant rise in BALF NO in the OVA group (2.377 ± 0.758) compared with NC group (1.303 ± 1.604) was significantly decreased by pregsal (1.823 ± 0.300) and MP (1.198 ± 0.330) (Fig. 1A).

3.1.3. Pregsal abolished delayed-type hypersensitivity

DTH is the response of T-cells against the antigen. There was a significant rise in DTH in OVA group rats (2.21 ± 0.15) compared

with the NC group (1.89 ± 0.13). Conversely, treatment with pregsal (1.99 ± 0.14) and MP (1.89 ± 0.11) significantly reduced DTH compared with the OVA group (Fig. 1B).

3.1.4. Pregsal abrogated the OVA-specific T-cell response

Through *ex vivo* experiments, T-cell proliferation was determined in isolated spleen cells from the four groups using 100 µg/ml OVA concentration. The proliferation of splenocytes, determined through uptake of BrdU, significantly increased in OVA group (0.447 ± 0.029) compared with the NC group (0.365 ± 0.027). Pregsal (0.371 ± 0.033) and MP (0.277 ± 0.044) significantly reduced splenocyte proliferation (Fig. 1C).

3.1.5. Pregsal arrested inflammatory cell infiltration in the lungs

Lung histopathology revealed that the infiltration of inflammatory cells in the OVA group (3 ± 0.53) was significantly enhanced compared with the NC group (0.75 ± 0.46). Treatment with pregsal (2.13 ± 0.35) and MP (1.63 ± 0.52) significantly lowered the inflammatory cell infiltration compared with OVA (Fig. 2A-E).

Table 2
Effect of pregsal on total and differential cell counts in blood and BALF.

Treatments	Total cell count in Blood ×10 ⁶ /ml	Differential cell count in Blood ×10 ⁶ /ml				
		Lymphocytes	Neutrophils	Eosinophils	Monocytes	Basophils
NC	5.86 ± 2.23	4.69 ± 1.87	0.13 ± 0.07	0.11 ± 0.05	0.87 ± 0.56	0.04 ± 0.04
OVA	31.74 ± 10.08 ^{###}	18.57 ± 5.05 ^{###}	6.91 ± 3.66 ^{###}	2.31 ± 0.59 ^{###}	3.16 ± 1.49 ^{###}	0.78 ± 0.47 ^{###}
Pregsal	14.37 ± 4.54 ^{***}	9.63 ± 3.04 ^{***}	2.08 ± 0.78 ^{***}	0.84 ± 0.25 ^{***}	1.63 ± 0.72 ^{**}	0.2 ± 0.07 ^{***}
MP	13.8 ± 2.96 ^{***}	9.46 ± 1.69 ^{***}	1.7 ± 0.81 ^{***}	0.61 ± 0.17 ^{***}	1.91 ± 0.45 [*]	0.14 ± 0.09 ^{***}
Treatments	Total cell count in BALF ×10 ⁶ /ml	Differential cell count in BALF ×10 ⁶ /ml				
		Lymphocytes	Neutrophils	Eosinophils	Macrophages	Basophils
NC	5.84 ± 0.62	1.4 ± 0.36	0.89 ± 0.10	0.14 ± 0.03	2.01 ± 0.23	0.13 ± 0.03
OVA	11.42 ± 1.516 ^{###}	3.34 ± 0.42 ^{###}	2.12 ± 0.39 ^{###}	1.01 ± 0.26 ^{###}	4.62 ± 0.69 ^{###}	0.22 ± 0.05 ^{###}
Pregsal	8.85 ± 1.35 ^{***}	2.17 ± 0.32 ^{***}	1.4 ± 0.22 ^{***}	0.59 ± 0.12 ^{***}	3.39 ± 0.67 ^{***}	0.15 ± 0.05 ^{**}
MP	8.28 ± 1.47 ^{***}	1.86 ± 0.38 ^{***}	1.27 ± 0.29 ^{***}	0.44 ± 0.12 ^{***}	2.89 ± 0.67 ^{***}	0.11 ± 0.04 ^{***}

Results are represented as mean ± SD (n = 10). P < 0.05, P < 0.01, and P < 0.001 are indicating *, **, and ***, respectively, for statistical difference compared with the OVA group. ### designates P < 0.001 for statistical difference in comparison with the NC group. Negative control (NC), ovalbumin (OVA), salicylaldehyde derivative of pregabalin (pregsal), methylprednisolone (MP), bronchoalveolar lavage fluid (BALF).

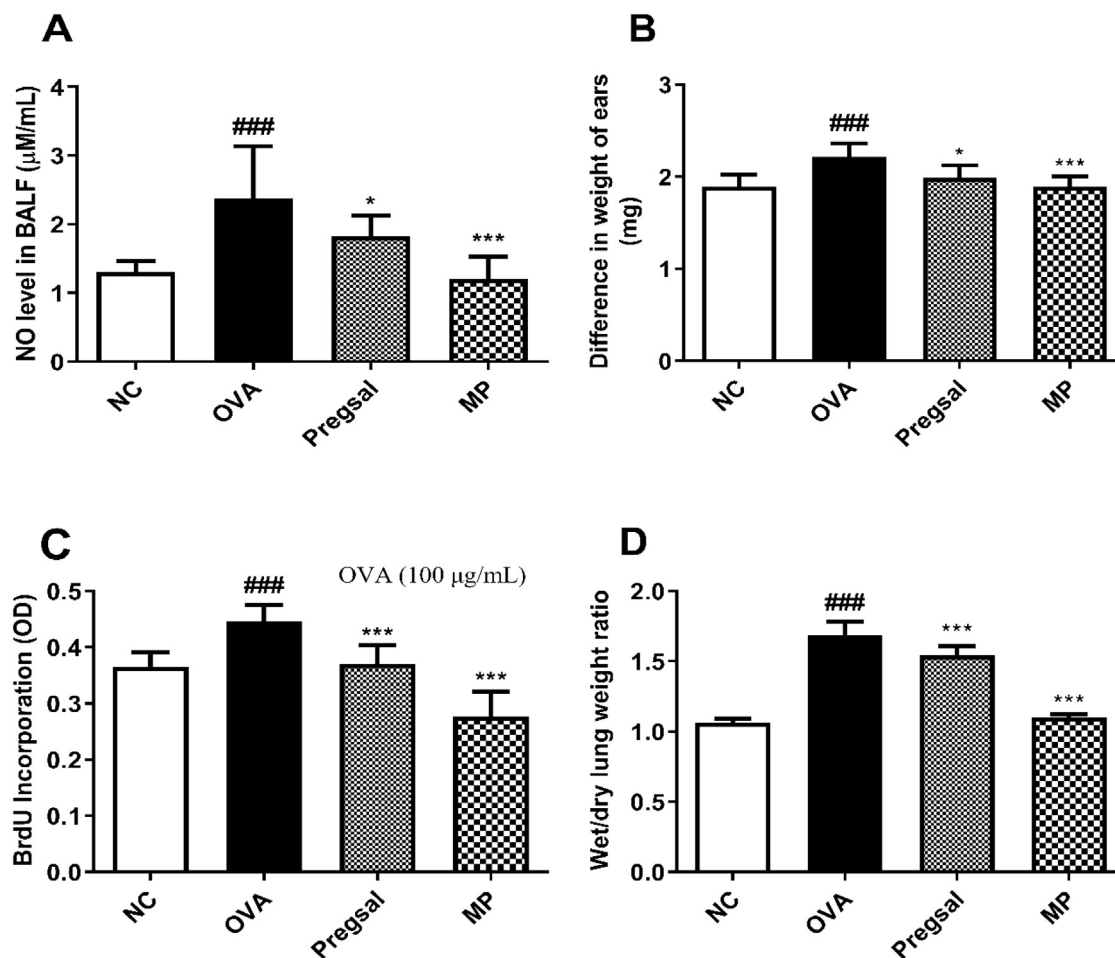


Fig. 1. The effect of pregalsal on inflammatory parameters. (A) Nitric oxide (NO) production in BALF. (B) Delayed-type hypersensitivity, represented by the difference in weight between right and left ear. (C) OVA-stimulated splenocyte proliferation. (D) Wet/dry lung weight ratio. Results are presented as mean \pm SD for 10 rats in each group. $P < 0.05$ and $P < 0.001$ are represented by * and ***, respectively, indicating statistical difference compared to the OVA group. ### denotes $P < 0.001$ for statistical difference compared to the NC group. Negative control (NC), ovalbumin (OVA), salicylaldehyde derivative of pregabaline (pregalsal), methylprednisolone (MP).

3.2. Effect of pregalsal on lung remodelling

3.2.1. Pregalsal alleviated wet/dry lung weight ratio

The wet/dry lung weight ratio was used to determine the severity of lung edema. There was a significant increase in lung wet/dry weight ratio in the OVA group (1.68 ± 0.10) compared with the NC group (1.07 ± 0.03). Pregalsal (1.54 ± 0.07) and MP (1.10 ± 0.02) significantly reduced the wet/dry weight ratio compared with the OVA group (Fig. 1D)

3.2.2. Pregalsal decreased epithelial wall thickness and goblet cell hyperplasia

A significant increase in lung epithelial wall thickness was seen in the OVA group (36.50 ± 2.75) compared with the NC group (12.38 ± 1.41). Pregalsal (19.75 ± 3.45) and MP (16.25 ± 3.69) significantly reduced epithelial thickness compared with the OVA group (Fig. 2A-D, F). The percentage of PAS-positive goblet cells was used to show goblet cell hyperplasia. The OVA group (2.63 ± 0.52) showed a significant increase in percentage goblet cells compared with the NC group (0.13 ± 0.35). This was attenuated with both pregalsal and MP with a significantly lowered PAS scoring of 1.63 ± 0.52 and 1.25 ± 0.46 , respectively (Fig. 3A-E).

3.2.3. Pregalsal reduced hydroxyproline level in lungs

The hydroxyproline level in rat lungs was used to estimate the total collagen. The results revealed a significant rise in lung

hydroxyproline in the OVA group (1.538 ± 0.221) compared with NC group (0.187 ± 0.036). Treatment with pregalsal (0.675 ± 0.167) and MP (0.279 ± 0.136) showed a marked decrease in lung hydroxyproline compared with the OVA group (Fig. 4A).

3.2.4. Pregalsal abolished arginase activity

The activity of arginase was significantly enhanced in the lungs of OVA-treated animals (3.789 ± 0.498) as compared to the NC group (1.331 ± 0.339). Arginase activity in the lungs was abolished after treatment with pregalsal (2.194 ± 0.382) and MP (1.303 ± 0.574) as compared to the OVA group (Fig. 4B).

3.2.5. Pregalsal reduced osteopontin (OPN) level

A significant escalation in lung OPN activity was seen in the OVA group (12.96 ± 2.20) compared with the NC group (5.18 ± 1.51). Conversely, treatment with pregalsal (9.82 ± 1.68) and MP (6.11 ± 2.15) significantly reduced OPN in the lung homogenate as compared to the OVA group (Fig. 4C).

3.2.6. Pregalsal decreased ornithine decarboxylase (ODC) activity

The results demonstrated a significant increase in lung mitochondrial ODC activity in the OVA group (4626 ± 1408) compared to the NC group (2374 ± 897.2). A significant reduction in mitochondrial ODC activity was found after treatment with pregalsal (3308 ± 562.5) and MP (2951 ± 452.2) as compared to the OVA group (Fig. 4D).

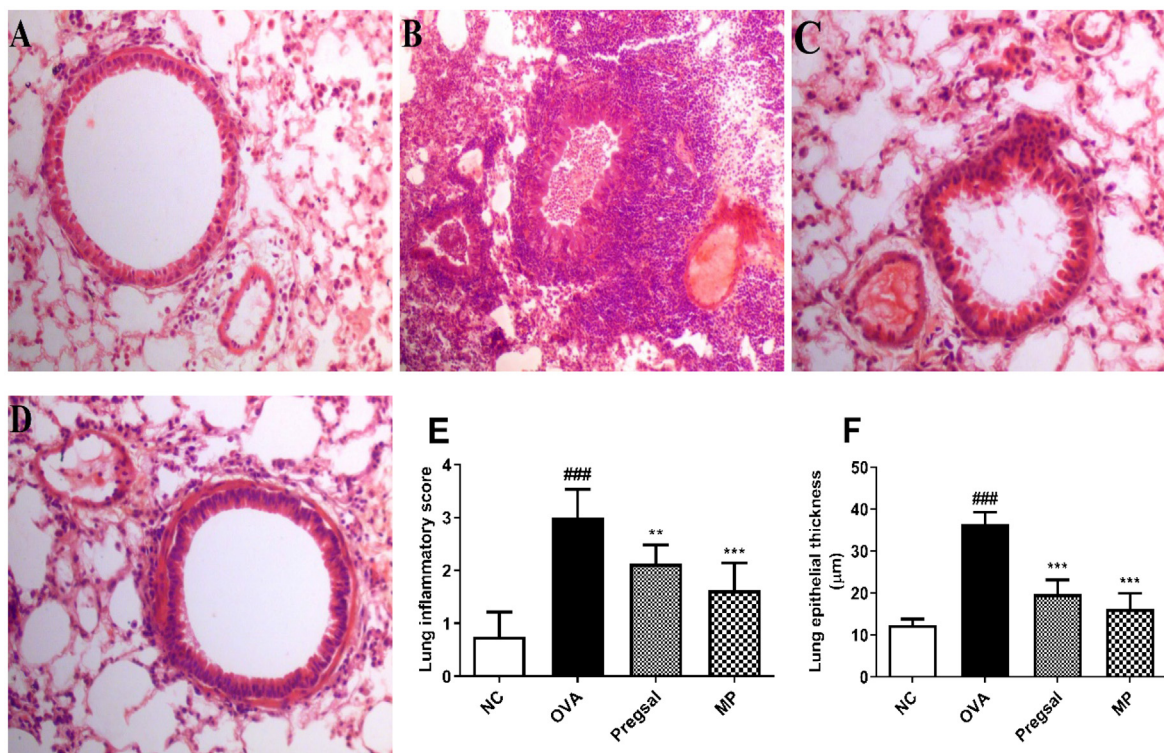


Fig. 2. Analysis of lung histology. Hematoxylin and Eosin (H&E) stain; 40X. (A) Represents a section of the lung from NC group showing no pathological changes. (B) Lung section from the OVA group with marked peribronchial, perivascular and interstitial inflammatory infiltrate, thickened bronchial basement membrane, vascular congestion and diffuse necroinflammatory exudate in the alveoli. (C) Treatment with pregasal showing a significant amelioration of inflammatory exudate and bronchial basement membrane thickening, also represented by images (E) and (F) showing marked reduction in the inflammatory score and lung epithelial thickness, respectively. (D) MP treatment shows significant amelioration of inflammatory exudate and bronchial basement membrane thickening. ### represents difference between NC and OVA group indicating $P < 0.001$. *** and ** denotes $P < 0.01$ and $P < 0.01$, respectively, which indicates significant difference compared with OVA group. Negative control (NC), ovalbumin (OVA), salicylaldehyde derivative of pregabalin (pregsal), methylprednisolone (MP).

3.3. Pregsal downregulated inflammatory mediators

Table 3 shows significant upregulation in the mRNA expression of TNF- α , NF- κ B, IL-4, IL-8, IL-13, arginase I, TGF- β , FGF2, CTGF and UII in OVA group compared with the NC group. Treatment with pregasal significantly reduced the mRNA expression of TNF- α , NF- κ B, IL-4, IL-8, IL-13, TGF- β , FGF2, CTGF, and UII compared with the OVA group, with the exception to arginase I which showed a non-significant reduction.

4. Discussion

In the current study, lung inflammation and remodelling were established by sensitizing the rats with OVA. These rats displayed a significant rise in inflammatory biomarkers of blood, BALF and lung tissue, along with upregulated inflammatory mediators and inflammatory cells infiltration. In response to the OVA challenge, the lung epithelial thickness was enhanced along with goblet cell hyperplasia and the release of various inflammatory mediators, including cytokines (Abdel Aziz et al., 2013). Other research has also demonstrated a similar response in OVA-induced model (Lee et al., 2012). While, treatment with pregasal and MP, significantly attenuated the OVA-induced inflammatory response.

Uncontrolled and excessive release of pro-inflammatory cytokines, known as a cytokine storm, is seen in various diseases, including rheumatic, allergic and infectious diseases, and tumor immunotherapy. Clinically, a cytokine storm presents enhanced inflammatory parameters, systemic inflammation and multiple organ failure (Zhang et al., 2020). Our results indicated that administration of pregasal significantly lowered the levels of inflammatory

mediators, including cytokines, chemokine and growth factors; consequently, targeting inflammatory mediators effectively attenuate the development of airway inflammation and lung remodelling (Lee and Yang, 2013).

Lung edema is a hallmark of airway inflammation (Tillie-Leblond et al., 2007). OVA-challenged rats demonstrated a significant rise in lung edema. In addition, Th2 cytokines play a role in eosinophil infiltration and recruitment of mast cells which further causes mucus hypersecretion and airway hyper-responsiveness (Singh et al., 2019). In the current investigation, pregasal reduced lung edema, probably by decreasing eosinophil infiltration via reducing the Th2 cytokines.

The contribution of NO in the pathogenesis of various diseases affecting the pulmonary system is well known (Barnes et al., 2010). The detection of exhaled NO is now a validated method in the management of respiratory diseases, including bronchial asthma (Prado et al., 2011). Augmented expression of inducible NO synthase (iNOS) in the airway epithelium of asthmatics may cause an increase in NO concentration (Abuelezz, 2018). Our results showed increased NO level in BALF of OVA group, which was significantly reduced by pregasal.

Hydroxyproline is used as an index of collagen synthesis. In the current study, the hydroxyproline synthesis increased more than tenfold in rats of the OVA group. Our results were in line with the earlier findings in which increased hydroxyproline was found in asthma and airway remodelling (Kim et al., 2016). The arginase pathway also contributes to proline production and lung fibrosis and in airway diseases, the role of arginase activity has been demonstrated (van den Berg et al., 2018). The product of arginase activity is L-ornithine which is further converted into putrescine

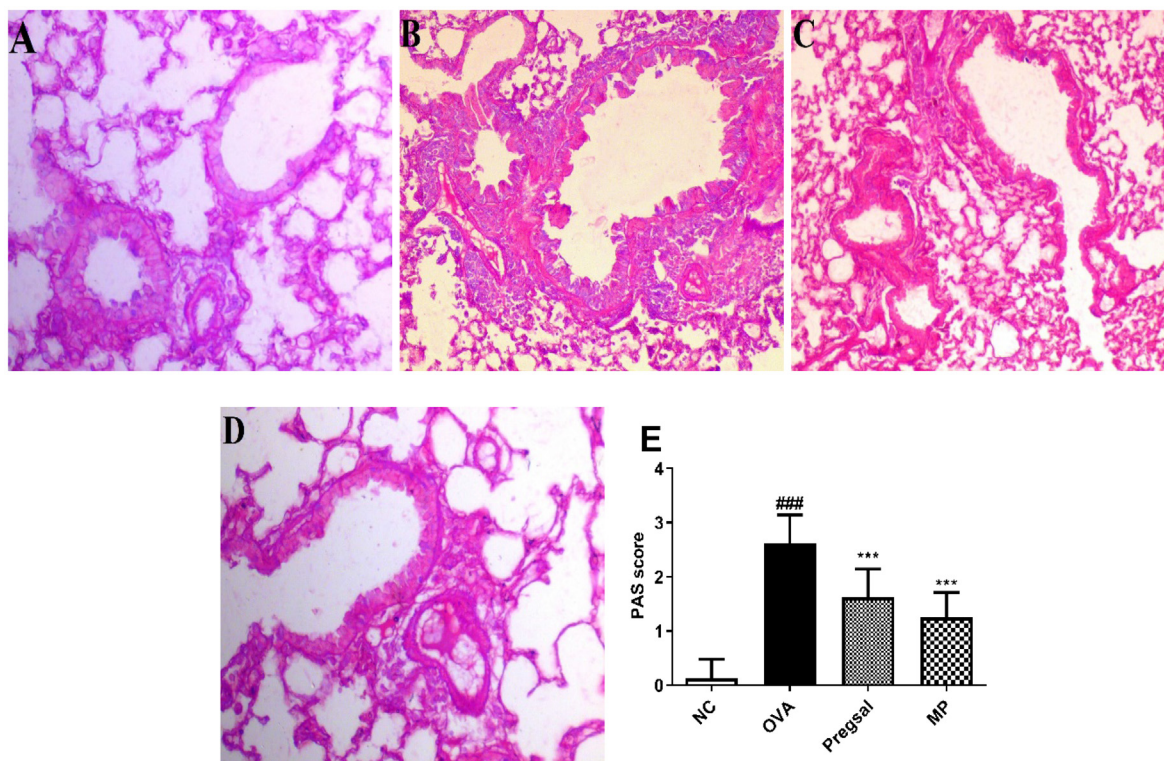


Fig. 3. Lung sections were obtained from all the groups and Periodic acid-Schiff (PAS) staining for the identification of goblet cell hyperplasia (40X). (A) Photomicrograph showing PAS staining of NC with single bronchial goblet cell epithelial lining. (B) OVA groups with marked goblet cell hyperplasia. (C) Photomicrograph showing treatment with pregal and (D) methylprednisolone significantly ameliorated the goblet cell hyperplasia. (E) Graphical representation of PAS scoring in all the groups where ### and *** indicate statistical difference as compared with NC and OVA group, respectively, at $P < 0.001$. Negative control (NC), ovalbumin (OVA), salicylaldehyde derivative of pregabalin (pregsal), methylprednisolone (MP).

with the help of an enzyme ODC (Latour et al., 2020). ODC activity may then be used as a measure of mitochondrial activity and oxidative stress. OVA-induced rats showed a higher hydroxyproline level, along with enhanced arginase and ODC activity, which were normalized with pregal. In a similar study, pharmacological inhibition of polyamine biosynthesis using α -difluoromethylornithine (an ODC inhibitor) significantly reduced airway responsiveness (North et al., 2013).

OPN is a glycoprotein that has been associated with airway inflammation and lung remodelling (Delimpoura et al., 2010). Our results revealed that OPN was upregulated in rat lung tissues of the OVA group. Previous *in vitro* and *in vivo* study have also demonstrated that many inflammatory cells such as T-cells, macrophages and eosinophils express OPN (Kohan et al., 2007). In the current study, pregal and MP significantly decreased OPN levels in lung tissue, aligning with previous research in which osteopontin deficiency protects against lung fibrosis and airway remodelling (Simoes et al., 2009).

Higher expression of TNF- α , NF- κ B, IL-4, IL-8, IL-13 and TGF- β were observed in the lungs of OVA group rats. However, treatment with pregal markedly reduced their mRNA expression levels. Previously, lower levels of TNF- α and IL-1 β have also been found in a pregabalin pretreatment group (Kazanci et al., 2016). Furthermore, in this study, pregal significantly suppressed NF- κ B, suggesting that pregal may inhibit the transcription activation of NF- κ B-dependent various genes of cytokines, chemokine and inflammatory mediators through interacting with the promoter of the NF- κ B responsive gene (Zhong et al., 2016).

Our study also showed down-regulation of profibrotic FGF2 and CTGF in the pregal treated group. FGF2 enhances the production of TGF- β , which contributes to the development of airway remod-

elling (Yang et al., 2012). Additionally, the mitogenic action of FGF2 has also been reported for endothelial cells, airway smooth muscle cells and fibroblasts, and its enhanced level has also supported the role of FGF2 in the lung remodelling process (Bissonnette et al., 2014). Moreover, enhanced protein expression of CTGF is directly correlated with increased eosinophils and total inflammatory cell count (Lin et al., 2017). In contrast, inhibition of CTGF expression can reverse the development of tissue remodelling and fibrosis (Lipson et al., 2012).

Previously, a considerable increase of UII protein and mRNA expression level has been observed in the lung of asthmatic rats compared with control and further *in vitro* study revealed that UII has the potential to act as a mitogen for airway smooth muscle cells and induce their proliferation through the upregulation of TGF- β (Zhang et al., 2012). Administration of UII in experimental rats resulted in enhanced TGF- β in hepatic cells (Kemp et al., 2009). Our results illustrate the upregulation of UII mRNA expression levels in the OVA group. However, Pregal treatment significantly attenuated the inflammatory response by inhibiting UII. This result suggested that pregal reduced the expression of UII and prevents airway remodelling by regulating the TGF- β expressions in the lungs.

There are some limitations to this study. In this study, OVA caused Th2 type allergic inflammation and lacks biological features of airway inflammation and lung remodelling caused by bacterial or viral infection. Airway inflammation and lung remodelling involves various pathways, and further *in vivo* and *in vitro* analysis of downstream signalling molecules such as Akt/PI3k, MAPKs and JNK are required for better understanding the effects of pregal on airway inflammation and lung remodelling.

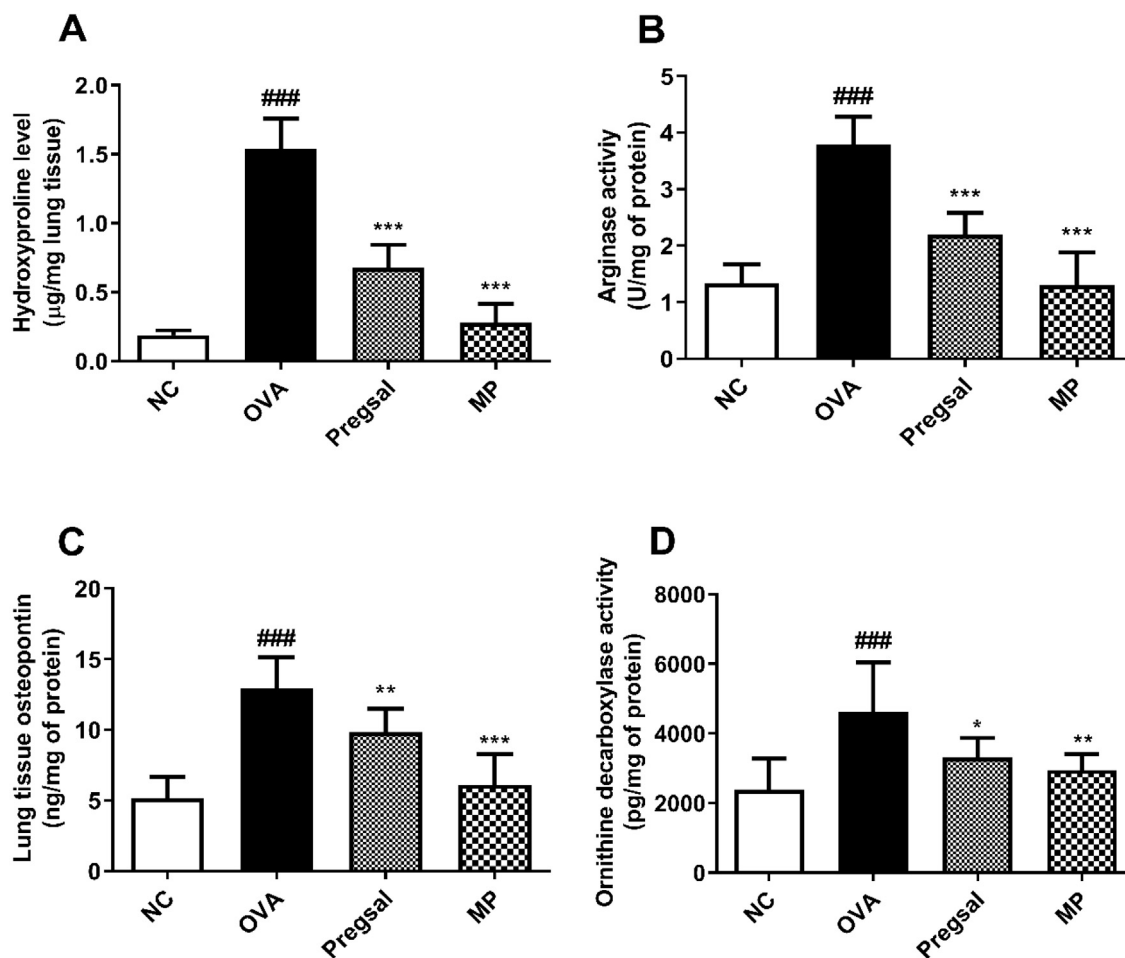


Fig. 4. The effect of pregalsal on lung remodelling parameters. (A) Hydroxyproline level. (B) Arginase activity. (C) Osteopontin level in lung tissues and, (D) Ornithine decarboxylase activity in lung mitochondria. Results are represented as mean \pm SD for 10 rats in each group. $P < 0.001$, $P < 0.01$ and $P < 0.05$ is denoted by *******, ****** and *****, respectively, which show a statistical difference in comparison to the OVA group. **###** denotes $P < 0.001$, which show a statistical difference in comparison to the NC group. Negative control (NC), ovalbumin (OVA), salicylaldehyde derivative of pregabalin (pregalsal), methylprednisolone (MP).

Table 3
Pregalsal downregulated cytokines, chemokine and inflammatory mediators.

Markers	NC	OVA	Pregalsal	MP
TNF- α	19.66 \pm 3.51	49.71 \pm 4.46 ^{###}	36.57 \pm 6.90 ^{***}	27.31 \pm 0.81 ^{***}
NF- κ B	23.64 \pm 5.49	46.53 \pm 5.13 ^{###}	32.15 \pm 6.54 ^{**}	23.81 \pm 5.04 ^{***}
IL-4	22.40 \pm 5.90	78.50 \pm 8.71 ^{###}	39.42 \pm 6.71 ^{***}	30.07 \pm 4.37 ^{***}
IL-8	9.88 \pm 3.50	47.04 \pm 6.52 ^{###}	28.94 \pm 8.05 ^{***}	14.01 \pm 4.09 ^{***}
IL-13	20.11 \pm 3.15	48.10 \pm 4.05 ^{###}	37.70 \pm 6.82 ^{**}	22.40 \pm 3.07 ^{***}
Arginase I	17.18 \pm 4.54	34.09 \pm 5.48 ^{###}	26.74 \pm 5.59	18.74 \pm 2.63 ^{***}
TGF- β	34.90 \pm 5.54	56.83 \pm 3.77 ^{###}	43.34 \pm 8.39 ^{**}	29.28 \pm 4.43 ^{***}
FGF2	38.52 \pm 10.92	59.69 \pm 7.50 ^{###}	44.12 \pm 10.43 [*]	40.11 \pm 6.58 ^{**}
CTGF	46.47 \pm 13.10	74.92 \pm 8.34 ^{###}	53.40 \pm 12.17 [*]	46.84 \pm 8.16 ^{**}
Ull	36.53 \pm 8.84	65.04 \pm 7.18 ^{###}	45.87 \pm 8.98 ^{**}	31.73 \pm 6.55 ^{***}

Results are represented as mean \pm SD for 06 rats in each group. $P < 0.05$, $P < 0.01$, and $P < 0.001$ are symbolized by *****, ******, and *******, respectively, which show a statistical difference compared with the OVA-challenged group. **###** denotes $P < 0.001$, which display a statistical difference compared to the NC group. Negative control (NC), ovalbumin (OVA), salicylaldehyde derivative of pregabalin (pregalsal), methylprednisolone (MP).

5. Conclusion

The results of this investigation demonstrate that pregalsal ameliorates OVA-induced airway inflammation and pathological changes of lung remodelling in rats by lowering inflammatory cell infiltration, inhibiting arginase, and reducing the activity of ODC, hydroxyproline and OPN levels. Furthermore, pregalsal inhibited

NF- κ B, which then caused the downregulation of inflammatory mediators including cytokines, chemokine, and profibrotic growth factors. In general, we observed pregalsal having a significant anti-inflammatory effect. There is a great potential to study and establish the role of pregalsal in other lung conditions involving a cytokine storm, including SARS-CoV-2 lung infections, the greatest challenge and threat the world is currently facing.

Acknowledgements

This study was conducted with partial support from Higher Education Commission, Islamabad, Pakistan. We are also thankful to Translational Research Institute (TRI), University of Queensland, Brisbane, Australia for providing technical facilities.

Declaration of competing interest

The authors declare that there is no potential conflict of interest regarding the authorship, research, and/or publication of this article.

References

- Abdel Aziz, R.R., Helaly, N.Y., Zalata, K.R., Gameil, N.M., 2013. Influence of inhaled beclomethasone and montelukast on airway remodeling in mice. *Inflammopharmacology* 21 (1), 55–66. <https://doi.org/10.1007/s10787-012-0127-7>.
- Abuelezz, S.A., 2018. Nebivolol attenuates oxidative stress and inflammation in a guinea pig model of ovalbumin-induced asthma: a possible mechanism for its favorable respiratory effects. *Can. J. Physiol. Pharmacol.* 96 (3), 258–265. <https://doi.org/10.1139/cjpp-2017-0230>.
- Ahmad, N., Subhan, F., Islam, N.U., Shahid, M., Rahman, F.U., Fawad, K., 2017. A novel pregabalin functionalized salicylaldehyde derivative afforded prospective pain, inflammation, and pyrexia alleviating propensities. *Arch. Pharm.* 350 (6), e201600365. <https://doi.org/10.1002/ardp.201600365>.
- Ashraf, M.I., Shahzad, M., Shabbir, A., 2015. Oxyresveratrol ameliorates allergic airway inflammation via attenuation of IL-4, IL-5, and IL-13 expression levels. *Cytokine* 76 (2), 375–381. <https://doi.org/10.1016/j.cyto.2015.09.013>.
- Barnes, P.J., 2013. New anti-inflammatory targets for chronic obstructive pulmonary disease. *Nat. Rev. Drug Discov.* 12 (7), 543–559. <https://doi.org/10.1038/nrd4025>.
- Barnes, P.J., Dweik, R.A., Gelb, A.F., Gibson, P.G., George, S.C., Grasemann, H., Pavord, I.D., Ratjen, F., Silkoff, P.E., Taylor, D.R., Zamel, N., 2010. Exhaled nitric oxide in pulmonary diseases. *Chest* 138 (3), 682–692. <https://doi.org/10.1378/chest.09-2090>.
- Bissonnette, É.Y., Madore, A.-M., Chakir, J., Laviolette, M., Boulet, L.-P., Hamid, Q., Bergeron, C., Maghni, K., Laprise, C., 2014. Fibroblast growth factor-2 is a sputum remodeling biomarker of severe asthma. *J. Asthma* 51 (2), 119–126. <https://doi.org/10.3109/02770903.2013.860164>.
- Delimpoura, V., Bakakos, P., Tselioui, E., Bessa, V., Hillas, G., Simoes, D.C.M., Papiris, S., Loukides, S., 2010. Increased levels of osteopontin in sputum supernatant in severe refractory asthma. *Thorax* 65 (9), 782–786. <https://doi.org/10.1136/thx.2010.138552>.
- Dong, C., Wang, G., Li, B.o., Xiao, K., Ma, Z., Huang, H., Wang, X., Bai, C., 2012. Anti-asthmatic agents alleviate pulmonary edema by upregulating AQP1 and AQP5 expression in the lungs of mice with OVA-induced asthma. *Respir. Physiol. Neurobiol.* 181 (1), 21–28. <https://doi.org/10.1016/j.resp.2011.12.008>.
- El-Naby, E., 2019. Potentiometric sensing platform for selective determination of Pregabalin in pharmaceutical formulations. *Open J. Anal. Bioanal. Chem.* 3, 049–056. <https://doi.org/10.17352/ojabc.000011>.
- Hirota, N., Martin, J.G., 2013. Mechanisms of Airway Remodeling. *Chest* 144 (3), 1026–1032. <https://doi.org/10.1378/chest.12-3073>.
- Kazanci, B., Ozdogan, S., Kahveci, R., Gokce, E.C., Yigitkanli, K., Gokce, A., Erdogan, B., 2016. Neuroprotective effects of pregabalin against spinal cord ischemia-reperfusion injury in rats. *Turk. Neurosurg.* <https://doi.org/10.5137/1019-5149.JTN.17959-16.1>.
- Kemp, W., Kompa, A., Phrommintikul, A., Herath, C., Zhiyuan, J., Angus, P., McLean, C., Roberts, S., Krum, H., 2009. Urotensin II modulates hepatic fibrosis and portal hemodynamic alterations in rats. *Am. J. Physiol. Liver Physiol.* 297 (4), G762–G767. <https://doi.org/10.1152/ajpgp.00127.2009>.
- Kim, S.W., Kim, J.H., Park, C.K., Kim, T.J., Lee, S.Y., Kim, Y.K., Kwon, S.S., Rhee, C.K., Yoon, H.K., 2016. Effect of roflumilast on airway remodelling in a murine model of chronic asthma. *Clin. Exp. Allergy* 46 (5), 754–763. <https://doi.org/10.1111/cea.12670>.
- M. Kohan R. Bader I. Puxeddu F. Levi-Schaffer R. Breuer N. Berkman Enhanced osteopontin expression in a murine model of allergen-induced airway remodelling *Clin. Exp. Allergy* 0 0 2007 070908091822001 ??? 10.1111/j.1365-2222.2007.02801.x
- Lambrecht, B.N., Hammad, H., 2015. The immunology of asthma. *Nat. Immunol.* 16 (1), 45–56. <https://doi.org/10.1038/ni.3049>.
- Latour, Y.L., Gobert, A.P., Wilson, K.T., 2020. The role of polyamines in the regulation of macrophage polarization and function. *Amino Acids* 52 (2), 151–160. <https://doi.org/10.1007/s00726-019-02719-0>.
- Lee, I.-T., Yang, C.-M., 2013. Inflammatory Signalings Involved in Airway and Pulmonary Diseases. *Mediators Inflamm.* 2013, 1–12. <https://doi.org/10.1155/2013/791231>.
- Lee, S.H., Eren, M., Vaughan, D.E., Schleimer, R.P., Cho, S.H., 2012. A Plasminogen Activator Inhibitor-1 Inhibitor Reduces Airway Remodeling in a Murine Model of Chronic Asthma. *Am. J. Respir. Cell Mol. Biol.* 46 (6), 842–846. <https://doi.org/10.1165/rcmb.2011-0369OC>.
- Lin, S.-C., Chou, H.-C., Chiang, B.-L., Chen, C.-M., 2017. CTGF upregulation correlates with MMP-9 level in airway remodeling in a murine model of asthma. *Arch. Med. Sci.* 3, 670–676. <https://doi.org/10.5114/aoms.2016.60371>.
- Lipson, K.E., Wong, C., Teng, Y., Spong, S., 2012. CTGF is a central mediator of tissue remodeling and fibrosis and its inhibition can reverse the process of fibrosis. *Fibrogenesis Tissue Repair* 5, S24. <https://doi.org/10.1186/1755-1536-5-S1-S24>.
- Liu, S., Zhi, Y., Ying, S., 2020. COVID-19 and Asthma: Reflection During the Pandemic. *Clin. Rev. Allergy Immunol.* 59 (1), 78–88. <https://doi.org/10.1007/s12016-020-08797-3>.
- McCracken, J.L., Veeranki, S.P., Ameredes, B.T., Calhoun, W.J., 2017. Diagnosis and Management of Asthma in Adults: A Review. *JAMA* 318, 279–290. <https://doi.org/10.1001/jama.2017.8372>.
- North, M.L., Grasemann, H., Khanna, N., Inman, M.D., Gauvreau, G.M., Scott, J.A., 2013. Increased Ornithine-Derived Polyamines Cause Airway Hyperresponsiveness in a Mouse Model of Asthma. *Am. J. Respir. Cell Mol. Biol.* 48 (6), 694–702. <https://doi.org/10.1165/rcmb.2012-0323OC>.
- Prado, C.M., Martins, M.A., Tibério, I.F.L.C., 2011. Nitric Oxide in Asthma Pathophysiology. *ISRN Allergy* 2011, 1–13. <https://doi.org/10.5402/2011/832560>.
- Rana, S., Shahzad, M., Shabbir, A., 2016. Pistacia integerrima ameliorates airway inflammation by attenuation of TNF- α , IL-4, and IL-5 expression levels, and pulmonary edema by elevation of AQP1 and AQP5 expression levels in mouse model of ovalbumin-induced allergic asthma. *Phytomedicine* 23 (8), 838–845. <https://doi.org/10.1016/j.phymed.2016.04.006>.
- M. Raza Asim M. Shahzad X. Yang Q. Sun F. Zhang Y. Han S. Lu Suppressive effects of black seed oil on ovalbumin induced acute lung remodeling in E3 rats 2010 *Wkly Swiss Med* 10.4414/sm.w.2010.13128
- Russell, B., Moss, C., Rigg, A., Van Hemelrijck, M., 2020. COVID-19 and treatment with NSAIDs and corticosteroids: should we be limiting their use in the clinical setting? *Eccancermedicallscience* 14. <https://doi.org/10.3332/eccancer.2020.1023>.
- Schrier, D., Taylor, C., 2002. Method for treating asthma using pregabalin.
- Shahzad, M., Yang, X., Raza Asim, M.B., Sun, Q., Han, Y., Zhang, F., Cao, Y., Lu, S., 2009. Black seed oil ameliorates allergic airway inflammation by inhibiting T-cell proliferation in rats. *Pulm. Pharmacol. Ther.* 22 (1), 37–43. <https://doi.org/10.1016/j.pupt.2008.11.006>.
- Simoes, D.C.M., Xanthou, G., Petrochilou, K., Panoutsakopoulou, V., Roussos, C., Gratziou, C., 2009. Osteopontin Deficiency Protects against Airway Remodeling and Hyperresponsiveness in Chronic Asthma. *Am. J. Respir. Crit. Care Med.* 179 (10), 894–902. <https://doi.org/10.1164/rccm.200807-1081OC>.
- Singh, B.K., Lu, W., Schmidt Paustian, A.M., Ge, M.Q., Koziol-White, C.J., Flayer, C.H., Killingbeck, S.S., Wang, N., Dong, X., Riese, M.J., Deshpande, D.A., Panettieri, R.A., Haczku, A., Kambayashi, T., 2019. Diacylglycerol kinase ζ promotes allergic airway inflammation and airway hyperresponsiveness through distinct mechanisms. *Sci. Signal.* 12, eaax3332. <https://doi.org/10.1126/scisignal.aax3332>.
- Tillie-Leblond, I., Gosset, P., Le Berre, R., Janin, A., Prangere, T., Tonnel, A.B., Guery, B. P.H., 2007. Keratinocyte growth factor improves alterations of lung permeability and bronchial epithelium in allergic rats. *Eur. Respir. J.* 30, 31–39. <https://doi.org/10.1183/09031936.00011606>.
- van den Berg, M.P., Meurs, H., Gosens, R., 2018. Targeting arginase and nitric oxide metabolism in chronic airway diseases and their co-morbidities. *Curr. Opin. Pharmacol.* 40, 126–133. <https://doi.org/10.1016/j.coph.2018.04.010>.
- Xu, Z., Shi, L., Wang, Y., Zhang, J., Huang, L., Zhang, C., Liu, S., Zhao, P., Liu, H., Zhu, L., Tai, Y., Bai, C., Gao, T., Song, J., Xia, P., Dong, J., Zhao, J., Wang, F.-S., 2020. Pathological findings of COVID-19 associated with acute respiratory distress syndrome. *Lancet Respir. Med.* 8 (4), 420–422. [https://doi.org/10.1016/S2213-2600\(20\)30076-X](https://doi.org/10.1016/S2213-2600(20)30076-X).
- Yang, Y.C., Zhang, N., Van Crombruggen, K., Hu, G.H., Hong, S.L., Bachert, C., 2012. Transforming growth factor- β 1 in inflammatory airway disease: a key for understanding inflammation and remodeling. *Allergy* 67 (10), 1193–1202. <https://doi.org/10.1111/j.1398-9995.2012.02880.x>.
- Zhang, W.-x., Liang, Y.-F., Wang, X.-M., Nie, Y., Chong, L., Lin, L., Chen, C., Li, C.-C., 2012. Urotensin upregulates transforming growth factor- β 1 expression of asthma airway through ERK-dependent pathway. *Mol. Cell. Biochem.* 364 (1-2), 291–298. <https://doi.org/10.1007/s11010-012-1229-7>.
- Zhang, W., Zhao, Y., Zhang, F., Wang, Q., Li, T., Liu, Z., Wang, J., Qin, Y., Zhang, X., Yan, X., Zeng, X., Zhang, S., 2020. The use of anti-inflammatory drugs in the treatment of people with severe coronavirus disease 2019 (COVID-19): The Perspectives of clinical immunologists from China. *Clin. Immunol.* 214, 108393. <https://doi.org/10.1016/j.clim.2020.108393>.
- Zhong, Z., Umehura, A., Sanchez-Lopez, E., Liang, S., Shalpour, S., Wong, J., He, F., Boassa, D., Perkins, G., Ali, S., McGeough, M., Ellisman, M., Seki, E., Gustafsson, A., Hoffman, H., Diaz-Meco, M., Moscat, J., Karin, M., 2016. NF- κ B Restricts Inflammation Activation via Elimination of Damaged Mitochondria. *Cell* 164 (5), 896–910. <https://doi.org/10.1016/j.cell.2015.12.057>.